# Inhomogeneous plasticity in polypropylene spherulites

**J. R. Dryden, D. M. Shinozaki* and M. Slywchuk**
*Faculty of Engineering Science, University of Western Ontario, London, Ontario N6A 5B9, Canada*
*(Received 19 June 1990; accepted 30 October 1990)*

The non-linearity of the bulk stress–strain curve in polypropylene has been modelled by considering the curvilinear elastic anisotropy implicit in the lamellar structure of the spherulite. The spherulite is assumed to yield progressively as the applied stress is increased. The shape of the plastic zone as a function of applied tensile strain within the spherulite is estimated by incorporating a suitable yield criterion. The tangential to radial stiffness ratio in the polypropylene spherulite is found to be ~3:1.

**(Keywords: spherulite; polypropylene; curvilinear anisotropy; stress–strain)**

## INTRODUCTION

Partially crystalline polymers such as polypropylene consist of two phases; the crystalline and the non-crystalline. Each phase has distinct mechanical properties, and the overall bulk deformation behaviour depends on the relative amounts and distributions of the two phases. The relationship between microstructure and mechanical properties in crystalline polymers is usually described in terms of the average properties of the phases which constitute the material. Simple volume fraction averages can qualitatively describe bulk properties: examples being Voigt or Reuss averages. The elastic behaviour of oriented partially crystalline polymers has been modelled by Ward in terms of an aggregate[1]. A review of such micromechanical modelling is given by McCullough and most such work deals with the elastic response of the material[2]. In metals, a classical problem is to relate the isotropic elastic properties of the bulk polycrystalline solid with the anisotropic elastic coefficients of the individual single crystals. A similar approach seems to be useful for spherulitic polymers. In attempts to construct more accurate micromechanical models for deformation in crystalline polymers, both the elastic and plastic inhomogeneity and anisotropies of the microstructure must be considered. In particular, the progressive change in the distribution of plasticity within the microstructure should be incorporated into any accurate model. Such modelling will have applications in a variety of areas, but in particular the examination of sub-critical crack growth in spherulitic solids.

The phenomenological evidence for the progressive changes in a spherulite during mechanical testing is extensive[3,4]. Spherulites deform inhomogeneously elastically and plastically. The elastic deformation of isolated single spherulites has been described earlier[5]. The spherulite consists of lamellae arranged in a spherically symmetric array. In polyethylene, the $c$-axis is oriented in the planes lying tangentially to the sphere and the $b$-axis is parallel to the radius. The calculated stiffness along the chain backbone is about 40 times larger than that parallel to the $a$ or $b$ axes[6]. The average stiffness in the tangential plane is therefore expected to be considerably greater than that in the radial direction within the spherulite. The elastic inhomogeneity in polyethylene spherulites was shown in earlier work to result in progressive yielding in the microstructure which is dependent on the elastic anisotropy ratio[7]. The stress–strain curve measured in a tensile test before the load maximum was shown to be related to the progressive yielding within the material[8]. Micromechanically this has been modelled in terms of a solid which is plastically inhomogeneous.

The present work extends the earlier one-dimensional models, which used polyethylene as the prototypical material, to tensile deformation of polypropylene, and uses the micromechanical model to estimate the elastic anisotropy within the spherulite from tensile stress–strain measurements. The model uses the elastic anisotropy of the spherulite as a parameter which can be varied to make the mechanical response of the model fit the observed stress–strain response.

The estimation of the elastic anisotropy is significant in the development of more accurate models of large strain yielding and plastic deformation in spherulitic materials. The experimental measurement of these anisotropies is not otherwise possible in bulk melt crystallized samples. Models which accurately represent the mechanical behaviour of spherulites are important in understanding the microstructural origins of strength in these materials.

## ELASTIC DEFORMATION OF A SPHERULITE

Macroscopically, the polymer appears to be elastically homogeneous and isotropic with two independent elastic parameters, Young's modulus $E$ and Poisson's ratio $v$. If these two parameters are known then any of the other properties, for example the bulk modulus $k$ and the shear modulus $\mu$, can be calculated by standard relations. On a finer scale, the microscopic detail becomes significant.

* To whom correspondence should be addressed

0032-3861/91/152760-06

Individual lamellae are highly anisotropic, with the stiffness parallel to the molecular axis being much greater than that perpendicular. Sectors of individual spherulites are not isotropic but rather highly anisotropic, with properties which are expected to be different in the radial and tangential directions, depending on the exact local lamellar orientation. In addition, amorphous regions lie between the lamellae, and between the radial arms of the spherulite. The net stiffness in any one direction, tangential or radial, is not possible to evaluate using standard models, since it depends on the details of the crystalline/non-crystalline microstructure, which is not known accurately enough.

The present model assumes each spherulite can be described elastically using curvilinear anisotropy. There are five independent elastic coefficients. The first step in the analysis is to relate the five spherulite coefficients to the bulk properties. The analysis, which is essentially of the so-called 'self-consistent' type, follows that described in detail earlier[9].

To examine the stresses within one spherulite, spherical coordinates are convenient (*Figure 1*). The body centre of the spherulite lies at the origin, and the $z$-axis is parallel to the polar axis while the equatorial plane is defined by the $xy$ plane. Such a spherulite is considered in this model to be embedded in an infinite and isotropic matrix (*Figure 2*). In the matrix, distant from the influence of the spherulite, the deformation is uniform and corresponds to uniaxial tension applied in the $z$ direction, that is, parallel to the polar axis. Near (and within) the spherulite, the uniform deformation field is of course

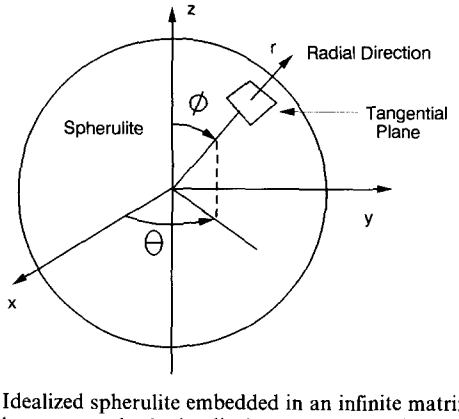


**Figure 1** Idealized spherulite embedded in an infinite matrix; $u$ is the radial displacement and $v$ is the displacement in the $\phi$ direction. The properties parallel to the tangential plane are different from those parallel to the radial direction

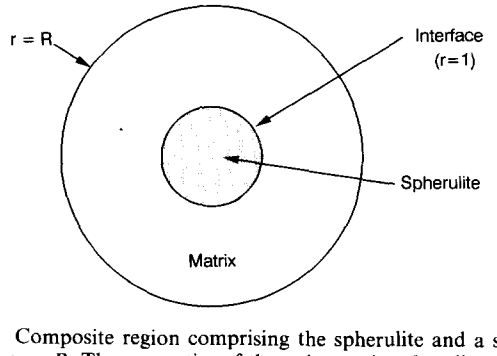


**Figure 2** Composite region comprising the spherulite and a shell of matrix $1 < r < R$. The properties of the anisotropic spherulite and the bulk are matched at the interface in the calculation

disturbed. To find the elastic field it is necessary to solve the basic elastic equations in the matrix and in the spherulite and then 'join' these solutions together with suitable boundary conditions at their interface (which we may take for convenience as being given by $r = 1$).

*The elastic field within the spherulite*

It is assumed that the elastic properties of the spherulite in the $\phi$ and $\theta$ directions are the same. Hooke's law is:

$$\begin{aligned}
\sigma_r &= C_{11}e_r + C_{12}e_\phi + C_{12}e_\theta \\
\sigma_\phi &= C_{12}e_r + C_{22}e_\phi + C_{23}e_\theta \\
\sigma_\theta &= C_{12}e_r + C_{23}e_\phi + C_{22}e_\theta \\
\tau_{r\phi} &= 2C_{44}e_{r\phi} \\
\tau_{r\theta} &= 2C_{44}e_{r\theta} = 0 \\
\tau_{\phi\theta} &= (C_{22} - C_{23})e_{\phi\theta} = 0
\end{aligned} \tag{1}$$

The shear stress components, $\tau_{r\theta}$ and $\tau_{\phi\theta}$, vanish because the problem is axisymmetric with respect to the $z$ direction.

Two differential equations involving the radial and tangential displacements, $u$ and $v$, can be obtained by inserting Hooke's law, along with the displacement strain relations, into the equilibrium equations. The details of this analysis are given elsewhere[9]. It is mathematically convenient to define $X = \cos\phi$ and make use of the well developed theory of spherical harmonics. Since the problem is axisymmetric, the zonal harmonics (Legendre polynomials) are prominent and, furthermore, since the deformation is symmetrical with respect to the equatorial plane only the zeroth and second harmonics are required:

$$\begin{aligned}
P_0(X) &= 1 \\
P_2(X) &= (3X^2 - 1)/2 \\
P_2^1(X) &= 3X\sqrt{1 - X^2}
\end{aligned}$$

At the matrix/spherulite interface the displacement, $(u, v)$ and the stress components, $\sigma_r$ and $\tau_{r\phi}$, are to be joined. These quantities, within the spherulite are:

$$\begin{aligned}
u &= Dr^\gamma P_0(X) + (b_1 Gr^\alpha + b_2 Hr^\beta)P_2(X) \\
v &= (Gr^\alpha + Hr^\beta)P_2^1(X) \\
\sigma_r &= b_0 Dr^{\gamma-1}P_0(X) + (b_3 Gr^{\alpha-1} + b_4 Hr^{\beta-1})P_2(X) \\
\tau_{r\phi} &= (b_5 Gr^{\alpha-1} + b_6 Hr^{\beta-1})P_2^1(X)
\end{aligned} \tag{2}$$

where $\gamma$, $\alpha$, $\beta$ and $b_0, \ldots, b_6$ are known in terms of $C_{11}, C_{12}, \ldots, C_{44}$. The coefficients $D$, $G$ and $H$ will be found eventually by connecting these expressions with those corresponding to the deformation in the matrix at $r = 1$.

*The elastic field in the matrix*

In the matrix, far from the spherulite, the strain components

$$e_x^A = e_y^A = -\nu e_z^A$$

correspond to uniaxial stress where the superscript A is intended to indicate the strain caused by the applied stress. The elastic field is given in most of the standard texts on the theory on elasticity[10,11]. The expressions

corresponding to equation (2) are:

$$u=\left(e_0^A r-\frac{A}{r^2}\right)P_0(x)+\left[e_2^A r+\left(\frac{5-4\nu}{1-2\nu}\right)\frac{C}{r^2}-\frac{3B}{r^4}\right]P_2(X)$$

$$v=-\left(\frac{e_2^A}{2}r+\frac{C}{r^2}+\frac{B}{r^4}\right)P_2^1(X)$$

$$\sigma_r=\left(3ke_0^A+\frac{4\mu A}{r^3}\right)P_0(X) \qquad (3)$$

$$+2\mu\left[e_2^A+\left(\frac{2\nu-10}{1-2\nu}\right)\frac{C}{r^3}+\frac{12B}{r^5}\right]P_2(X)$$

$$\tau_{r\phi}=-2\mu\left[\frac{e_2^A}{2}+\left(\frac{1+\nu}{1-2\nu}\right)\frac{C}{r^3}-\frac{4B}{r^5}\right)P_2^1(X)$$

where $e_0^A=(e_z^A+2e_x^A)/3$ is the hydrostatic strain component, $e_2^A=2(e_z^A-e_x^A)/3$ is the deviatoric strain, and $\mu$ and $k$ are, respectively, the shear and bulk moduli.

*Interface conditions*

At the interface, $r=1$, the corresponding expressions in (2) and (3) are equated. By virtue of the orthogonal properties of the zonal harmonics we obtain two sets of relations. First, between $A$ and $D$, it is found that:

$$\begin{pmatrix}\frac{1}{b_0} & \frac{1}{-4\mu}\end{pmatrix}\begin{pmatrix}D\\A\end{pmatrix}=e_0^A\begin{pmatrix}1\\3k\end{pmatrix} \qquad (4)$$

Second, between the coefficients $G$, $H$, $C$ and $B$ it is found that:

$$\begin{pmatrix} b_1 & b_2 & -\frac{5-4\nu}{1-2\nu} & 3\\ b_3 & b_4 & -2\mu\frac{2\nu-10}{1-2\nu} & -24\mu\\ 1 & 1 & 1 & 1\\ b_5 & b_6 & 2\mu\frac{1+\nu}{1-2\nu} & -8\mu\end{pmatrix}\begin{pmatrix}G\\H\\C\\B\end{pmatrix}=e_2^A\begin{pmatrix}1\\2\mu\\-1/2\\-\mu\end{pmatrix} \qquad (5)$$

The uniaxial deformation has effectively been split into hydrostatic and deviatoric components. The interface conditions, (4), are due to the hydrostatic portion of the applied deformation and are decoupled from the conditions, (5), set by the deviatoric component.

*Relationship between the spherulite and bulk properties*

*Figure 2* shows the spherulite embedded in an infinite matrix. Consider the elastic energy of the composite that is contained in the spherical region bounded by $R$. If the deformation is axisymmetric, the elastic energy can be found by integrating one half $(u\sigma_r+v\tau_{r\phi})$ over the spherical surface defined by $R$. The strain energy, $W$, of the spherulite–matrix composite, evaluated from this integral is:

$$W=\left[\left(\frac{\sigma_z^A e_z^A}{2}\right)\left(\frac{4\pi R^3}{3}\right)\right]$$

$$-\left[\pi\left((8\mu+6k)e_0^A A-12\mu\frac{1-\nu}{1-2\nu}e_2^A C\right)\right] \qquad (6)$$

The first term on the right represents the strain energy due to uniaxial stress $\sigma_z^A$ applied to a homogeneous volume equal to $4\pi R^3/3$. The second term on the right-hand side represents the change in strain energy caused by the spherulite.

Using Cramer's rule it is possible to obtain, from (4) and (5), expressions for the coefficients $A$ and $C$. The coefficient $B$, perhaps surprisingly, does not affect the energy of the composite region. If the spherulite elastic properties are completely unrelated to those of the matrix the coefficients $A$ and $C$ will be non-zero and the elastic energy will be changed according to equation (6). On the other hand, if we relate the two sets of elastic properties, by demanding that the strain energy of the system must remain constant, then, from equation (6), we must impose the condition that the coefficients $A=C=0$. By forcing the condition $A=0$ in (4), we obtain the relation:

$$\det\begin{pmatrix}1 & 1\\ b_0 & 3k\end{pmatrix}=0 \qquad (7)$$

so that

$$k=\frac{b_0}{3}$$

$$=\frac{1}{3}\left[2C_{12}-\frac{C_{11}}{2}+\frac{1}{2}\sqrt{C_{11}^2+8C_{11}(C_{22}+C_{23}-C_{12})}\right]$$

Similarly, using (5) and setting $C=0$, we obtain:

$$\det\begin{pmatrix} b_1 & b_2 & 1 & 3\\ b_3 & b_4 & 2\mu & -24\mu\\ 1 & 1 & -1/2 & 1\\ b_5 & b_6 & -\mu & -8\mu\end{pmatrix}=0 \qquad (8)$$

so that the shear modulus $\mu$ can then be found by taking the positive root of the quadratic defined in (8).

The macroscopic properties are usually given in terms of $E$ and $\nu$. The shear and bulk moduli are proportional to $E$:

$$\mu=\frac{E}{2(1+\nu)} \qquad k=\frac{E}{3(1-2\nu)}$$

The value of $\nu$ is typically around 1/3 so that $k\cong E$ and $\mu\cong 3E/8$.

## ELASTIC CONSTANTS FOR DIFFERENT ANISOTROPY RATIOS

The elastic constants for a spherulite radial segment can be estimated for different tangential/radial anisotropy ratios. Assuming a specific anisotropy ratio ($C_{22}/C_{11}$), where $C_{11}$ is the stiffness parallel to the radial direction, and $C_{22}$ is that in the tangential plane, the remaining elastic constants ($C_{12}$, $C_{22}$, $C_{44}$) can be calculated from relations (7) and (8). The results are shown in *Table 1*, scaled with the average tensile modulus $E$. The materials which are numbered 1–4 are those with tangential stiffness greater than the radial, listed in increasing degree of anisotropy. Those materials with radial stiffness greater than the tangential are listed as materials 5–8. For comparison, the isotropic case is also listed.

## YIELD AND INHOMOGENEOUS PLASTICITY

The stress–strain curve for spherulitic polymers is non-linear at small strains below the load maximum. The spherulite is elastically inhomogeneous, and as the applied tensile stress increases in a mechanical test, the

**Table 1** Elastic constants for a variety of anisotropy ratios $k = E$ and $\mu = 3E/8$

| Number | $C_{22}/C_{11}$ | $C_{11}/E$ | $C_{12}/E$ | $C_{22}/E$ | $C_{23}/E$ | $C_{44}/E$ |
|---|---|---|---|---|---|---|
| 1 | 2 | 1.0 | 0.7 | 2.0 | 0.780 | 0.250 |
| 2 | 3 | 1.0 | 0.50 | 3.0 | 0.500 | 0.073 |
| 3 | 5 | 1.0 | 0.1 | 5.0 | 0.422 | 0.018 |
| 4 | 10 | 1.0 | −1.0 | 10.0 | 4.000 | 0.011 |
| Isotropic | 1 | 3/2 | 3/4 | 3/2 | 3/4 | 3/8 |
| 5 | 1/2 | 2.0 | 0.9 | 1.0 | 0.860 | 1.600 |
| 6 | 1/3 | 3.0 | 0.8 | 1.0 | 0.827 | 0.800 |
| 7 | 1/5 | 5.0 | 0.6 | 1.0 | 0.824 | 0.580 |
| 8 | 1/10 | 10.0 | 0.7 | 1.0 | 0.628 | 0.380 |

yield stress is reached locally at different applied stresses so plasticity is initiated progressively through the spherulite. This has been experimentally observed earlier in polyethylene[12] and in polypropylene[13]. For polypropylene, the large strain plastic deformation is accommodated by microcracking in the polar regions of the spherulite and by plastic shear in the equatorial regions (where the tensile axis is parallel to the polar direction)[14]. The regions of the spherulite which plastically yield can be predicted in terms of the distribution of stress in the spherulite. An approximate analysis based on this micromechanical description can be made by calculating the distribution of stress elastically. Using an appropriate yield condition defined in terms of the state of stress, the regions of the spherulite which have yielded can be identified.

Yield in polymers shows a dependence upon the hydrostatic component of the applied stress. Significant increases in tensile yield stress are observed for applied hydrostatic pressures which are of the same order of magnitude as the yield stress of the material[15,16]. To account for this the yield criterion may be written as follows (in terms of the stress invariants):

$$I_2 + \alpha I_1 = c \tag{9}$$

where $\alpha$ and $c$ are material properties. The invariant $I_1$ is the sum of the normal stresses and the second term therefore represents the effect of the hydrostatic pressure upon yield; $I_2$ is the equivalent stress, which includes the shear components and is the only significant term for materials which show no pressure dependence.

Using data from Mears *et al.*[15], Zok[17] has estimated the relevant parameters for polypropylene as $\alpha = 0.061$ and $c = 22.6$ MPa. These values have been used in the present calculations. The slope of the tensile stress–strain curve gave stiffness value $E = 500$ MPa.

## PROGRESSIVE YIELDING AND THE SHAPE OF THE STRESS–STRAIN CURVE

If we consider one of the materials listed in *Table 1*, in the early portion of the loading curve, the stress within a typical spherulite is given by Hooke's law, equation (1), and it will vary with position in the spherulite. For the tangentially stiff materials (materials 1–4 in *Table 1*) the stresses tend to be largest near the periphery of the sphere, while for the radially stiff materiasls (materials 5–8) the stresses are largest near the centre of the spherulite. The magnitude of this stress concentration increases with the degree of spherulite anisotropy.

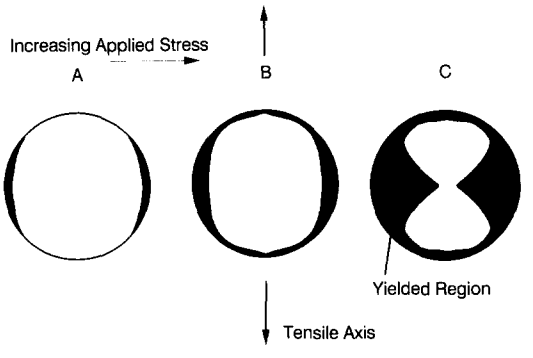


**Figure 3** Development of the yielded region for the tangentially stiff polymer number 2 ($C_{22}/C_{11} = 3/1$). The boundary between the yielded (shaded) and the unyielded regions changes with increasing applied stress (A, B and C). The corresponding points on the stress–strain curve are labelled in *Figure 5*. The plastic zone starts at the outer regions of the equatorial region and moves inwards

In a tensile test, the elastic stresses increase inhomogeneously within the spherulite until the yield criterion given by equation (9) is reached locally. Within each spherulite contours of $(I_2 + \alpha I_1)$ can be plotted and plastic yield will occur where these contours attain their largest value. The shape of the plastic zone within the spherulite is given approximately by the contour equal to $c$. The relaxation in stress field resulting from yielding of some parts of the spherulite is not included in the model calculation. This is similar to the treatment given in elementary approaches to fracture which predict the shape of the plastic zone ahead of the crack tip based upon the Westergaard solution for the stresses. Thus for materials 1–4, yield is initiated at the outer boundary and progressively moves inwards towards the spherulite centre as the applied stress increases (*Figure 3*). Conversely, for radially stiff materials (materials 5–8), yield is initiated near the centre of the spherulite and gradually moves towards the outer boundary (*Figure 4*).

The partially yielded spherulite consists of two 'phases': a yielded volume fraction ($f$), with a stiffness of $E_y$; and an unyielded volume fraction $(1 - f)$, with a stiffness $E$. For a Voigt solid, each phase carries equal strain and the composite modulus $E_c$ is given by:

$$E_c = E(1 - f) + E_y Y$$

The tensile stress–strain curve for polypropylene shows no work hardening after gross yielding, which is similar to an elastic-perfectly plastic solid. This suggests that the yielded fraction of the spherulite has a zero effective stiffness (an increase in applied strain does not result in

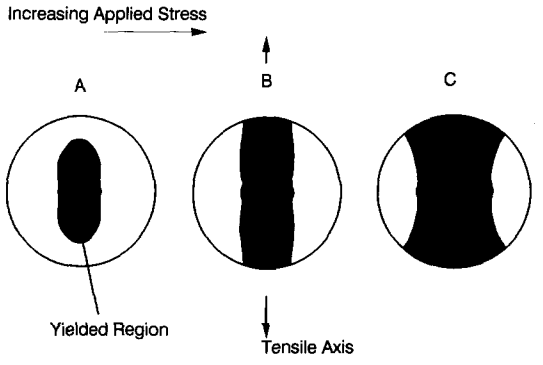


**Figure 4** Development of the yielded region for the radially stiff polymer number 8 ($C_{22}/C_{11} = 1/10$). The shape of the yielded zone is different from the tangentially stiff case in *Figure 3*. The points A, B and C correspond to the similarly labelled points on the stress–strain curve (*Figure 6*). The plastic zone starts at the centre of the spherulite and remains highly localized in the polar directions

an increase in stress) and $E_y$ is zero. Hence the bulk stiffness is reduced to $(1-f)E$. As the applied strain increases, the volume fraction which has yielded increases, and the incremental stiffness of the spherulite decreases. The applied stress–strain curve is therefore expected in this model to show curvature (a decreasing slope with increasing strain).

By determining the elastic-plastic boundary at different strains, the plastic volume fraction can be estimated and the effective spherulite stiffness calculated. The stress–strain curve for a tensile test can thus be predicted for each material listed in *Table 1*. The comparison between the predictions for the various anisotropy ratios and experimental curves for polypropylene are shown in *Figures 5* and *6* for spherulites with relatively high tangential stiffness and with high radial stiffness, respectively. A comparison with *Figures 3* and *4* shows the distribution of plasticity for three strains in cases which closely approximate the experimental curves.

A salient point to note is the difference in plastic zone development for the tangentially stiff and radially stiff models. The first case shows initial yielding in the equatorial regions, near the outer boundary of the spherulite. With increasing applied stress the plastic zone grows inwards. The radially stiff model (*Figure 4*) shows quite a different behaviour, with the initial yielded zone being at the centre of the spherulite and growing outwards towards the polar regions. This is qualitatively expected since a radially stiff spherulite transmits the matrix stress efficiently to the centre of the spherulite. The small values of applied strain at which yielding is observed in these models ($\sim 1\%$ in each case, at the point A), are consistent with the assumption that the material is effectively a linear elastic-inhomogeneous plastic solid. Earlier observations on stress relaxation experiments in these materials are consistent with plastic deformation being measurable at strains of $<5\%$[13]. Microstructural manifestations of this plasticity are not expected to be observable in these early stages of deformation since the plastic strains are small and are largely reversible on unloading.

## MICROSTRUCTURE OF POLYPROPYLENE AND THE MICROMECHANICAL MODEL

The comparison of the tensile stress–strain curves which are predicted from this model with the experimental curve (*Figures 5* and *6*) shows that the model is sensitive to the anisotropy ratio. The materials which most clearly match the observed behaviour are numbered 2 and 8. For radially stiff spherulites, the calculated curve approaches the measured one as the anisotropy ratio $C_{22}/C_{11}$ (tangential/radial) becomes very small (1/10). For tangentially stiff spherulites, the model predicts a best fit for a ratio of 3/1.

The lamellar structure in a spherulite has been described by Khoury as cross-hatched, with lamellar normals oriented approximately parallel to the radial direction, and in the tangential plane[18]. The stiffness ratio $C_{22}/C_{11}$, which is expected to be related to the *c*-axis orientation, is therefore not directly predictable from the local lamellar texture alone. However, the microstructural changes reported for polypropylene tested to large strains in tension show that crystallographic slip in the equatorial sectors is accompanied by microcracking in the polar sectors[14]. By comparing these observations with the predicted plastic zones shown in *Figures 3* and *4* for the two models which best fit the tensile stress–strain curves, it is clear that material number 2, with the anisotropy ratio of 3/1, is the most appropriate model.

The calculations support earlier work which suggested that inhomogeneous plasticity can account for the shape of the tensile stress–strain curve in spherulitic polymers[8,12,13]. The anisotropy ratio, which is controlled by

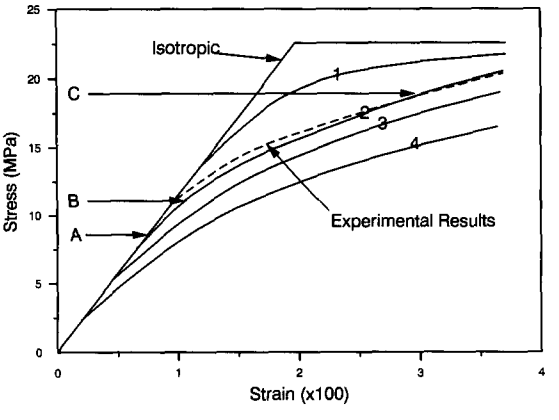


**Figure 5** Comparison between the experimental and calculated results for spherulites with relatively high tangential stiffness: numbers 1–4 in *Table 1*. The best fit is found for material 2 for $C_{22}/C_{11} = 3/1$

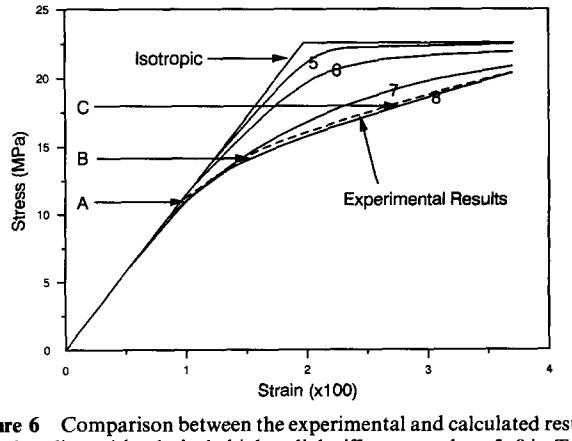


**Figure 6** Comparison between the experimental and calculated results for spherulites with relatively high radial stiffness: numbers 5–8 in *Table 1*. The best fit is found for material 8 for $C_{22}/C_{11} = 1/10$

the lamellar microstructure, has been shown to affect the bulk mechanical response directly. An important implication of this kind of calculation lies in the possibility of predicting microstructures susceptible to subcritical crack growth in cases such as environmentally assisted fracture, creep and fatigue. The approach shown here can be used to estimate this anisotropy ratio in bulk crystallized polymers.

## CONCLUSIONS

Using an elastic analysis, the stresses within a spherulite in a melt-crystallized solid have been calculated for an applied tensile stress. The model assumes an isolated spherulite embedded in a matrix. The matrix has the average isotropic properties of the bulk, while the spherulite has 'self-consistent' properties which are different in the radial and tangential directions, consistent with the known lamellar structures in polypropylene. The calculation involved considering the elastic field first within the spherulite and second within the matrix. The two fields were then joined at the interface, using appropriate criteria. The resultant stress fields within the spherulite could then be calculated accurately.

A suitable yield criterion was then invoked and the regions which have gone plastic were calculated as a function of applied strain. The volume fraction of plastically deformed material increased with applied strain, and the resultant tensile stress–strain curve was calculated. The curves for a variety of different tangential/radial stiffness ratios were compared to an experimental curve, and the best fits were found for ratios of $C_{22}/C_{11}$ of 1/10 and 3/1. The elastic anisotropy ratio for a spherulite could therefore be estimated for the first time.

## ACKNOWLEDGEMENTS

Support from the Natural Sciences and Engineering Research Council of Canada is gratefully acknowledged. Some assistance was obtained from the Ontario Center for Materials Research through A. E. Hamielec and J. D. Embury. A number of the central ideas of this work originated from discussions with C. M. Sargent.

## REFERENCES

1 Ward, I. M. 'Mechanical Properties of Solid Polymers', Wiley Interscience, New York, 1971
2 McCullough, R. L. 'Treatise on Materials Science and Technology', (Ed H. Herman), Vol. 10, Academic Press, New York, 1977, p. 453
3 Bassett, D. C. 'Principles of Polymer Morphology', Cambridge University Press, Cambridge, 1981, p. 234
4 Arridge, R. G. C. 'Mechanics of Polymers', Clarendon Press, Oxford, 1975
5 Dryden, J. R., Deakin, A. S. and Shinozaki, D. M. *J. Mech. Phys. Solids* 1986, **34**, 81
6 Odajima, A. and Maeda, M. *J. Polym. Sci.* 1966, **C15**, 55
7 Dryden, J. and Shinozaki, D. *J. Mater. Sci. Eng.* 1986, **84**, 105
8 Sargent, C. M. and Shinozaki, D. M. *Scripta Metall.* 1977, **11**, 401
9 Dryden, J. R. *J. Mech. Phys. Solids* 1988, **34**, 477
10 Timoshenko, S. P. and Goodier, J. N. 'Theory of Elasticity', McGraw-Hill, New York, 1970
11 Love, A. E. H. 'Mathematical Theory of Elasticity', Dover Publications, New York, 1944
12 Ibrahim, N., Shinozaki, D. M. and Sargent, C. M. *J. Mater. Sci. Eng.* 1977, **30**, 175
13 Shinozaki, D. M., Sargent, C. M. and Fehr, S. *J. Mater. Sci. Eng.* 1981, **51**, 93
14 Zok, F. and Shinozaki, D. M. *J. Mater. Sci.* 1987, **22**, 3995
15 Mears, D. R., Pae, K. D. and Sauer, J. A. *J. Appl. Phys.* 1969, **40**, 4229
16 Spitzig, W. A., Sober, R. J. and Richmond, O. *Acta Metall.* 1975, **23**, 885
17 Zok, F. *ME Sci Thesis* University of Western Ontario, 1985
18 Khoury, F. *J. Natl. Bur. Stand.* 1966, **70A**, 29